TRIAXIAL SHEAR TESTS ON SIMULATED SIERRA WHITE FAULT GOUGE & BOREHOLE SIMULATION IN SIERRA WHITE GRANITE

1. Triaxial Shear Tests on Simulated Sierra White Fault Gouge

Specimen Preparation

Laboratory shear tests were conducted on pulverized Sierra White granite (SWG) to investigate slip mechanisms in naturally occurring faults. Synthetic fault geometries were constructed by sandwiching fine grained SWG powder in between steel forcing blocks. For dry experiments, ~3.5 g of SWG powder was poured onto the face of the lower steel forcing block and leveled. For saturated experiments, enough fluid was added to the ~3.5 g of Sierra White granite powder to form a slurry. This slurry was applied to the lower forcing block and leveled. Inclined forcing blocks with 25.4 mm diameter and 35° faces, which were machined from ground steel rods with fine teeth on the faces, help to hold the gouge in place and prevent delamination at the interface. The top forcing block had a 2.03 mm centered hole to allow pore fluid access to the gouge. A fine steel mesh prevented back flow of the gouge into pore fluid lines. Samples were isolated from the confining medium using three layers of heat shrink polyolefin, as shown in Figure 1. The outer layer was shrunk over the o-rings on the end caps to form an impermeable seal, which was reinforced with steel tie wires on both sides of the o-rings. Hardened steel spacers and copper shim stock was placed between the steel forcing blocks and the end caps to preserve the parallelism of the Hastelloy wetted parts. For dry samples, the end caps were plugged, while the end caps for the saturated samples were connected to pore lines.

Experimental Setup and Test Procedure of Direct Shear Tests

The experimental setup for the triaxial shear test is shown in Figure 2. Figure 2 shows a Isopar-pressurized

chamber with an axial loading ram in a conventional loading machine. The jacketed rock specimen is placed inside the chamber, where it is loaded triaxially. The hydraulic intensifier applied a confining pressure via pressurized fluid to generate a normal stress on sample. The shear load was imposed on the specimen by advancing the axial ram at a constant displacement rate.

During the experiments, 15 MPa confining pressure, P_C, was applied to the sample before 5 MPa pore pressure, P_P, to generate 10 MPa effective pressure, P_E, where

$$P_E = P_C - P_P. \quad (1)$$

The confining pressure was increased to 80 MPa at a rate of 2.5 MPa/min while pore pressure was held constant to apply an effective pressure of 75 MPa. A differential stress of 1 kN was applied to the sample, and the axial ram was displaced at sequential constant rates of 36, 3.6, 0.36, 36, 360, and 36 mm/hr. The loads were obtained from an internal load cell, confining pressure from a pressure transducer mounted on the intensifier, and pore pressure from a syringe pump.

The procedure for the direct shear tests involved the following steps:

(a) A Sierra White gouge sample was prepared.

(b) The jacketed fault specimen was placed inside the vessel, and the vessel was sealed.

(c) A target effective pressure (e.g., 75 MPa) was applied first to the sample and was held throughout the experiment.

(d) The axial load was applied to the rock specimen by imposing a constant displacement rate of 0.36 to 360 mm/hr.

Test Results: Mechanical Behavior and Geophysical Response of Saturated Granite Joints

Three shear experiments were performed on two dry gouge samples and one saturated sample. Due to the experimental geometry, application of effective pressure, P_E, increased the normal stress, σ_n, while the

application of an axial stress, σ_A, increased both the normal stress and the shear stress, τ, as follows:

$$\tau = (\sigma_A - P_C)\sin\theta\cos\theta \quad (2)$$

and

$$\sigma_n = P_C + (\sigma_A - P_C)\sin^2\theta \quad (3)$$

where θ is the angle of the face of the forcing blocks (= 35°). Coefficient of friction is the ration between shear stress and normal stress

$$\mu = {}^{\tau}/_{\sigma_n}. \quad (4)$$

As the sample deforms, the inclination of the frictional interface causes the forcing blocks to move laterally as well as vertically, changing the true area of contact for the fault gouge. The reduction in contact area can be corrected by

$$A/A_0 = \Theta - \sin\Theta/\pi \quad (5)$$

and

$$\Theta = \pi - 2\sin^{-1}[(dl/2r)\tan\theta] \quad (6)$$

where r is the radius of the cylinder, dl is the axial displacement, and Θ is the angle of the inclined face. True normal and shear stress are the uncorrected values divided by A/A_0.

Coefficient of friction: dry vs. saturated

Overall, three shear tests were conducted from effective pressures (P_E) from 15 to 75 MPa. Figure 3 shows the coefficient of friction and shear displacement rate as a function of shear displacement. The coefficient of friction is higher for lower effective pressure. The saturated test at 75 MPa P_E has similar results to the dry test at the same conditions. Effects of shear displacement rate changes are observed in all tests, as the coefficient of friction temporarily drops with decreases in the rate and temporarily increases with increases in the rate.

Shear stress versus shear displacement for all three specimens are shown in Figure 4. Despite having a high coefficient of friction, the shear stress is much lower for the 15 MPa P_E test. Differences from rate changes are muted. Shear stress increases with increasing confinement. Shear stress results are similar for the 75 MPa P_E tests, wet and dry. At higher displacements, shear stress drops slightly for dry samples compared to saturated samples.

Conclusions

Friction experiments were successfully conducted on pulverized Sierra White granite for a range of effective pressures, displacement rates, and saturation states. Measured coefficients of friction are within the expected range for silicate rocks. Behavior with rate changes is consistent with rate and state friction formulations to enable calculations of *A-B* parameters for modeling inputs (reference???).

References

1. Belzer, B. D., & French, M. E. (2022). Frictional constitutive behavior of chlorite at low shearing rates and hydrothermal conditions. *Tectonophysics*, *837*, 229435.
2. Byerlee, J. (1978). Friction of rocks. *Rock friction and earthquake prediction*, 615-626.
3. Chester, F. M. (1994). Effects of temperature on friction: Constitutive equations and experiments with quartz gouge. *Journal of Geophysical Research: Solid Earth*, *99*(B4), 7247-7261.
4. Dieterich, J. H. (1979). Modeling of rock friction: 1. Experimental results and constitutive equations. *Journal of Geophysical Research: Solid Earth*, *84*(B5), 2161-2168.
5. Ruina, A. (1983). Slip instability and state variable friction laws. *Journal of Geophysical Research: Solid Earth*, *88*(B12), 10359-10370.
6. Scott, D. R., Lockner, D. A., Byerlee, J. D., & Sammis, C. G. (1994). Triaxial testing of Lopez

fault gouge at 150 MPa mean effective stress. *pure and applied geophysics*, *142*, 749-775.

7. Tembe, S., Lockner, D. A., & Wong, T. F. (2010). Effect of clay content and mineralogy on frictional sliding behavior of simulated gouges: Binary and ternary mixtures of quartz, illite, and montmorillonite. *Journal of Geophysical Research: Solid Earth*, *115*(B3).

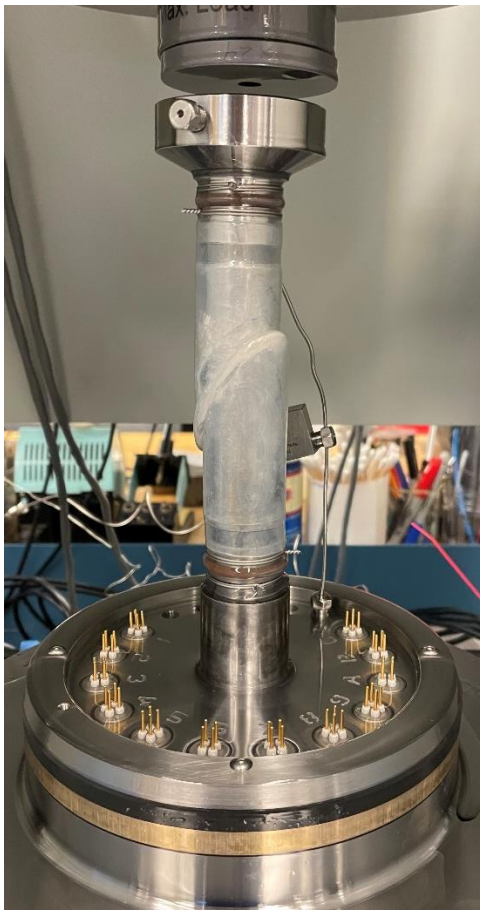

Figure 1. A deformed sample after shear test. A gauge along 35 degree slope inside a heat-shrink jacket is visibly shown.

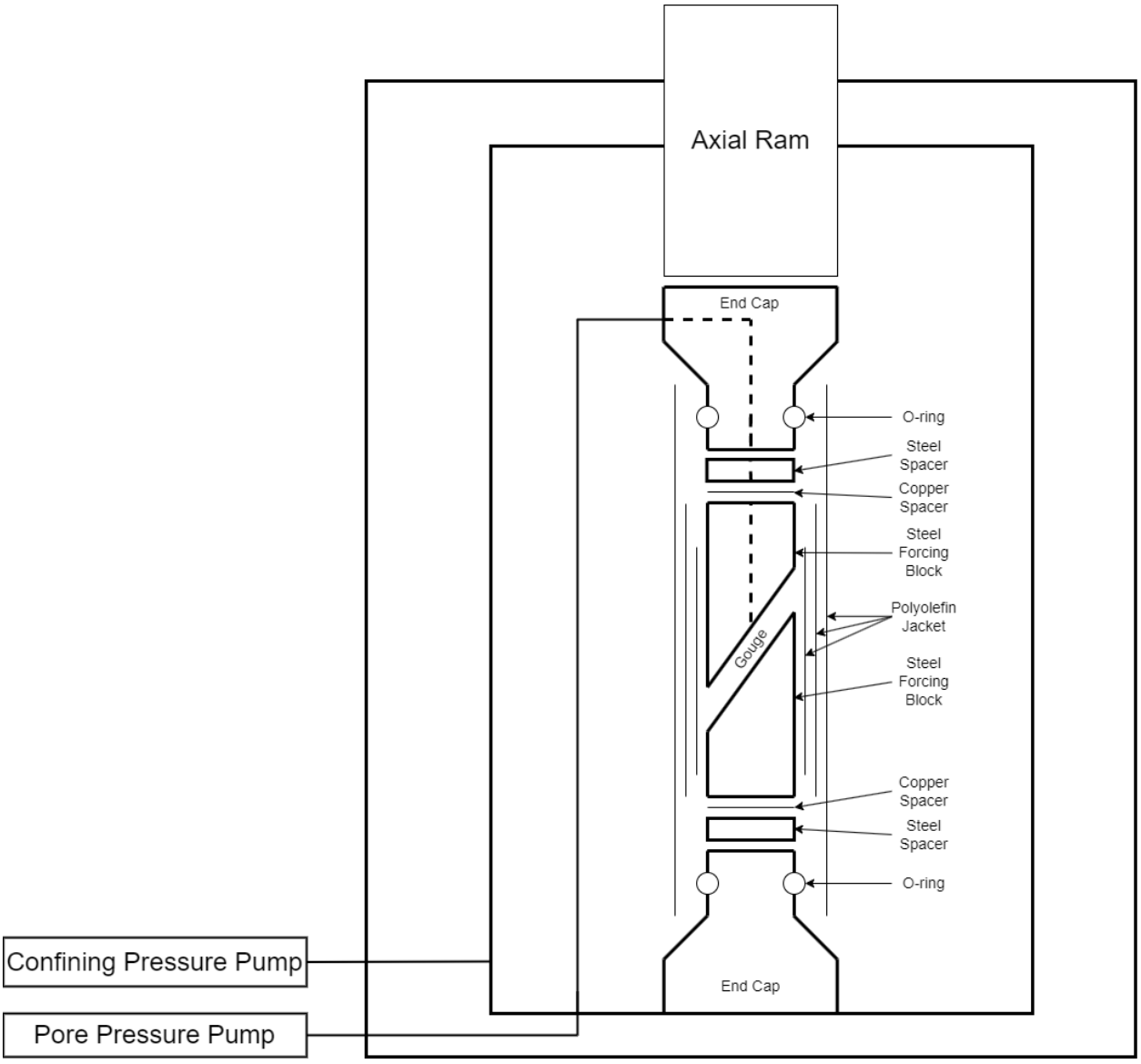

Figure 2. Experimental setup for triaxial shear tests.

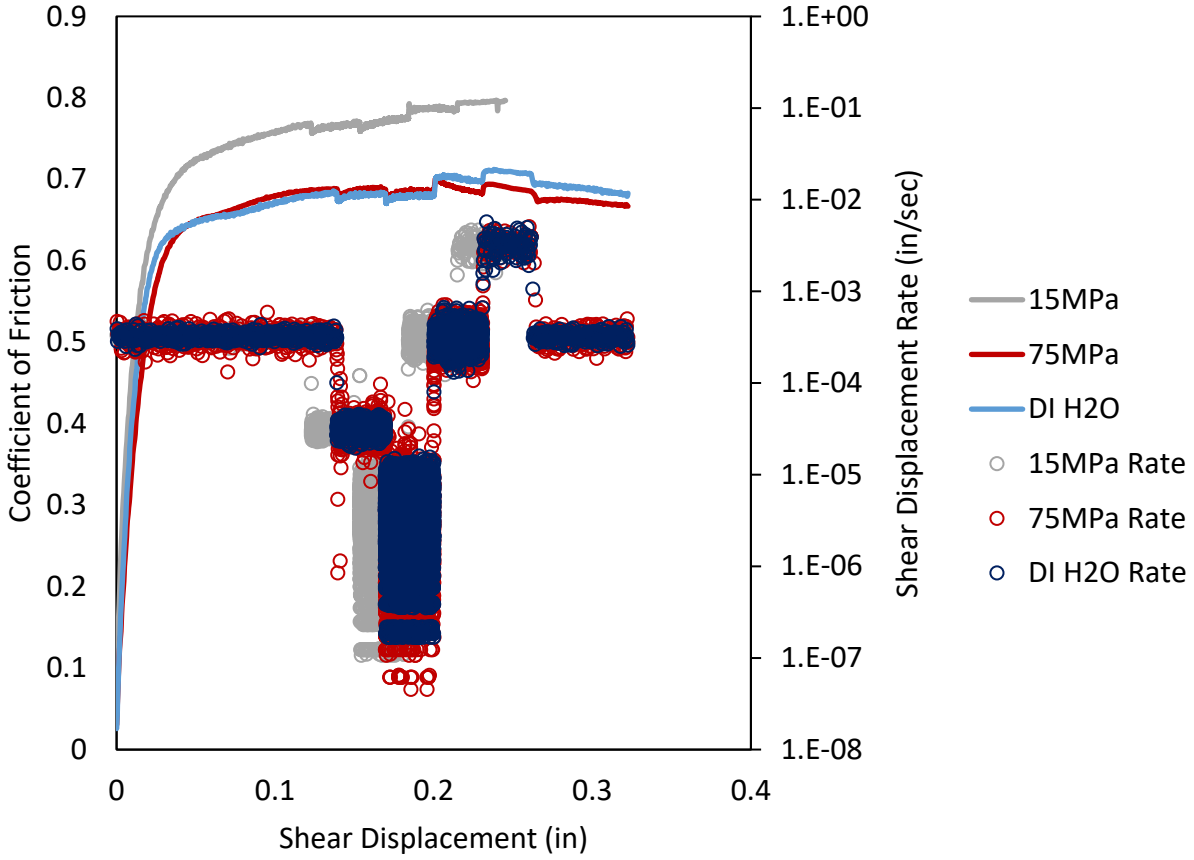

Figure 3. Coefficient of friction and shear displacement rate versus shear displacement under three different experiments. 15 MPa and 75 MPa rates were performed under dry condition and DI H_2O rate was performed at 75 MPa under water-saturated (wet) condition.

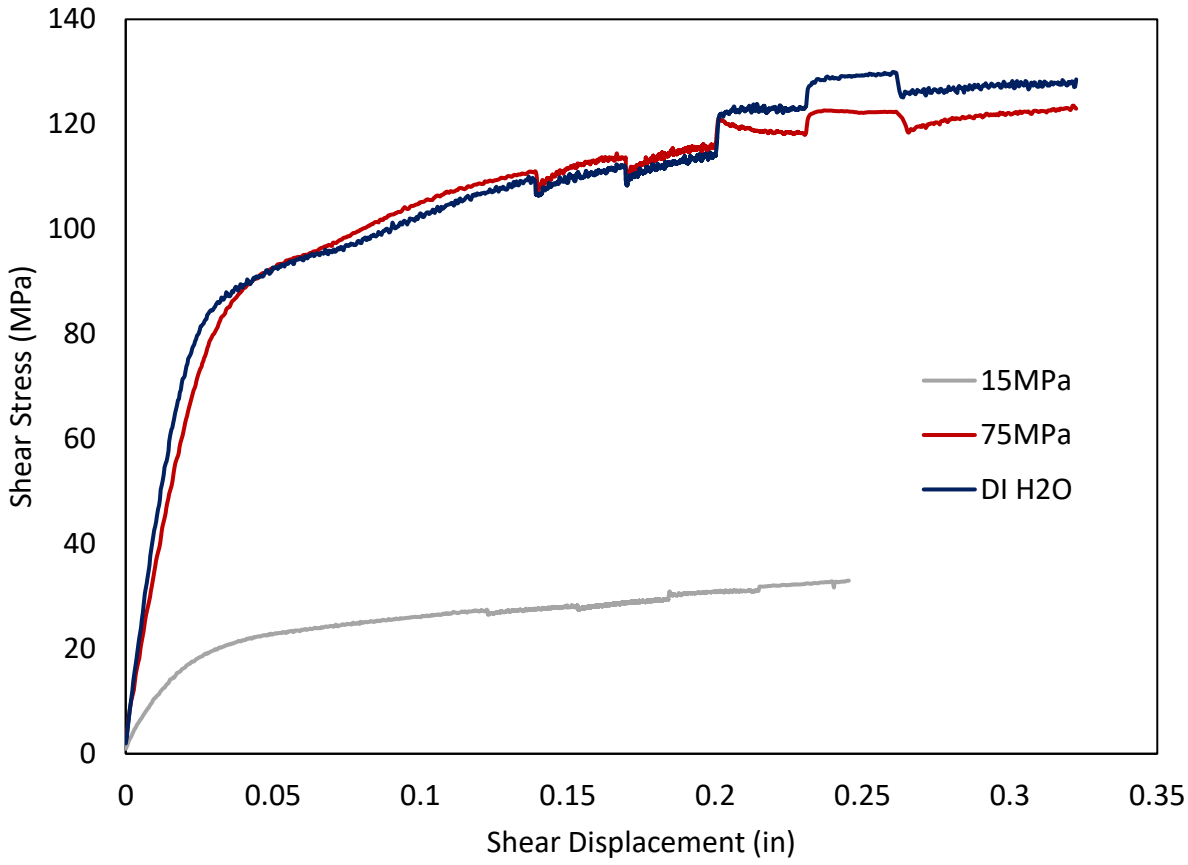

Figure 4. Shear stress versus shear displacement.

2. Borehole Stimulation Experiment

Borehole Specimen Preparation

Borehole breakout experiments at a laboratory scale were conducted on Sierra White granite (SWG) samples to evaluate the fracture initiation and propagation from a geothermal borehole. Simulated boreholes were created by drilling a small hole through the center of a cylindrical sample of SWG (Figure 5). This geometry utilizes the axial loading ram and confining pressure to create a differential stress around the borehole, as opposed to classic borehole simulations that required multiple rams to achieve similar stress states. The simulated borehole is isolated from the confining medium using ported steel covers, allowing for the independent pressurization of the borehole interior with different fluid chemistries. We followed an experimental procedure developed in our previous works (Choens et al., 2017, 2018, 2019) where this experimental geometry has been utilized to investigate bedding effects on borehole breakout development, load path effects on damage development around boreholes, and chemistry effects on borehole strength. Samples are jacked with a UV cure polyurethane to isolate the sample from the confining medium. Granite cylinders are 54 mm in diameter and ~95 mm long, and drilled borehole has a 11 mm diameter.

Experimental Setup and Test Procedure of Borehole Simulation Tests

The experimental setup for borehole breakout testing is shown in Figure 6. Figure 6 shows a Isopar-pressurized vessel with an axial loading ram in a conventional loading machine. The jacketed sample (Figure 5) is placed inside the chamber, where it is first loaded hydrostatically. The differential loading is imposed on the specimen by the axial loading ram with a constant displacement rate. Piezoelectric shock pins are mounted in 4 pin arrays on either side of the borehole (i.e., a total of 8 pins) to monitor and locate cracking using an acoustic emission data acquisition system during deformation.

During saturated experiments, fluid is introduced into the borehole via the pore lines and ported steel cover

after the application of a nominal confining pressure. For these experiments, pore pressure, P_P, is maintained at a constant value. After the application of confining pressure, P_C, both confining pressure and pore pressure are maintained at constant values to maintain a constant effective pressures, P_E in Eq. (1).

Confining pressure was increased at a rate of 1 MPa/min to the desired value. For dry experiments, confining pressure was increased to 17.2 MPa, for saturated experiments, confining pressure was increased to 20.6 MPa with 3.4 MPa applied pore pressure. Samples were deformed axially at a rate of 1.19% axial strain/hour. SWG-01 was deformed at 1.19 mm/hour due to lack of LVDT instrumentation. The loads were obtained from an internal load cell, confining pressure from a pressure transducer mounted on the intensifier, and pore pressure from a syringe pump. The normal load, the shear load and the slip displacement were monitored. The loads were obtained from strain gauges, attached to the tips of the loading shafts, placed inside the chamber to measure the actual load imposed and thus evaluate any friction that may develop between the chamber seals and the shafts. The displacements were measured by an external LVDT, and for SWG-02, displacements were monitored by internal LVDTs mounted to the sample. During the tests, seismic signals were captured during the test when signals crossed a digital threshold..

The procedure for the borehole simulation tests involved the following steps:

(e) A Sierra White cylinder was prepared with centered borehole and ported covers.

(f) The jacketed fault specimen was placed inside the vessel, and the vessel was sealed.

(g) A target effective pressure of 75 MPa was applied first to the sample and was held throughout the experiment.

(h) The axial load was applied to the rock specimen by imposing a constant displacement rate of 1.19%/hour.

Test Results: Mechanical Behavior and Geophysical Response of Saturated Granite Joints

Borehole simulation tests were performed on two samples, SWG-01 and SWG-02. SWG-01 and SWG-02 were performed under dry conditions and with deionized water as a pore fluid, respectively. The experimental geometry can be simplified to 2-D where the central borehole can be modeled as a hole in a semi-infinite plate. Using this approach, the stress distribution around the hole can be calculated using Kirsch's solutions (Kirsch, 1898). The stress acting along the borehole in the horizontal plane, σ_{BH}, is:

$$\sigma_{BH} = 3 * \sigma_A - P_C - P_P \quad (7)$$

where σ_A is the axial stress P_C is the confining pressure, and P_P is pore pressure inside the borehole. The stress along the borehole in the vertical plane, σ_{BV}, is:

$$\sigma_{BV} = 3 * P_C - \sigma_A - P_P. \quad (8)$$

σ_{BH} creates a maximum compressive stress around the borehole, and σ_{BV} creates a minimum, tensile stress around the borehole.

Axial strength: dry vs. saturated

Table 1 summarizes the results of borehole simulation tests on SWG. Figure 7 shows the differential stress as a function of axial strain. Results are compared against previous testing at similar conditions for dry SGW (Choens et al., 2018). SGW samples for the current experiments and previous experiments in Choens et al. (2018) were prepared from the same quarry. Behavior was found to be similar for all experiments conducted at the same effective pressure. Failure strength is similar for dry and saturated samples, as observed in previous work (Choens et al., 2018).

Stresses around the borehole are shown in Figures 8-9 and listed in Table 1. Calculated stresses reach maximum values upwards of 700 MPa, and tensile stresses reach values near -200 MPa. Post-test examinations of boreholes show that failure occurs along the horizontal plane of the borehole, or where the maximum compressive stresses occur as shown in Figure 10.

Borehole breakout tests were successfully conducted for a range of different saturation states, i.e. wet vs. dry. Observed borehole behavior is consistent with earlier testing.

References

8. Choens, R. C., Ingraham, M. D., Lee, M., & Dewers, T. A. (2017). Novel experimental techniques to investigate wellbore damage mechanisms. In *AGU 2017 Fall Meeting Abstracts* (T14C-08).
9. Choens, R. C., Ingraham, M. D., Lee, M. Y., Yoon, H., & Dewers, T. A. (2018). Acoustic emission during borehole breakout. In *52nd US Rock Mechanics/Geomechanics Symposium*. ARMA 18–0619. https://www.osti.gov/servlets/purl/1502282.
10. Choens, R. C., Lee, M. Y., Ingraham, M. D., Dewers, T. A., & Herrick, C. G. (2019). Experimental studies of anisotropy on borehole breakouts in Mancos Shale. *Journal of Geophysical Research: Solid Earth*, *124*(4), 4119-4141.
11. Jaeger, J.C. and Cook N.G.W. (1979). Fundamentals of Rock mechanics. 3rd Edition, Chapman and Hall, London, 1979.
12. Kirsch, J. H. (1898). The Theory of Elasticity and Requirements of the Science of Strength of Materials. *Journal of the Society of German Engineers*, *42*, 797-810.

Table 1. Summary of the peak shear strength of dry and saturated Sierra White granite (SWG) joints.

Conditions	Specimen	Peak differential strength (MPa)	Mean Stress (MPa)	Maximum borehole stress (MPa)	Minimum borehole stress (MPa)
Dry	Previous	205	74	648	-170
	SWG-01	221	91	698	-187
Saturated	SWG-02	208	90	664	-166

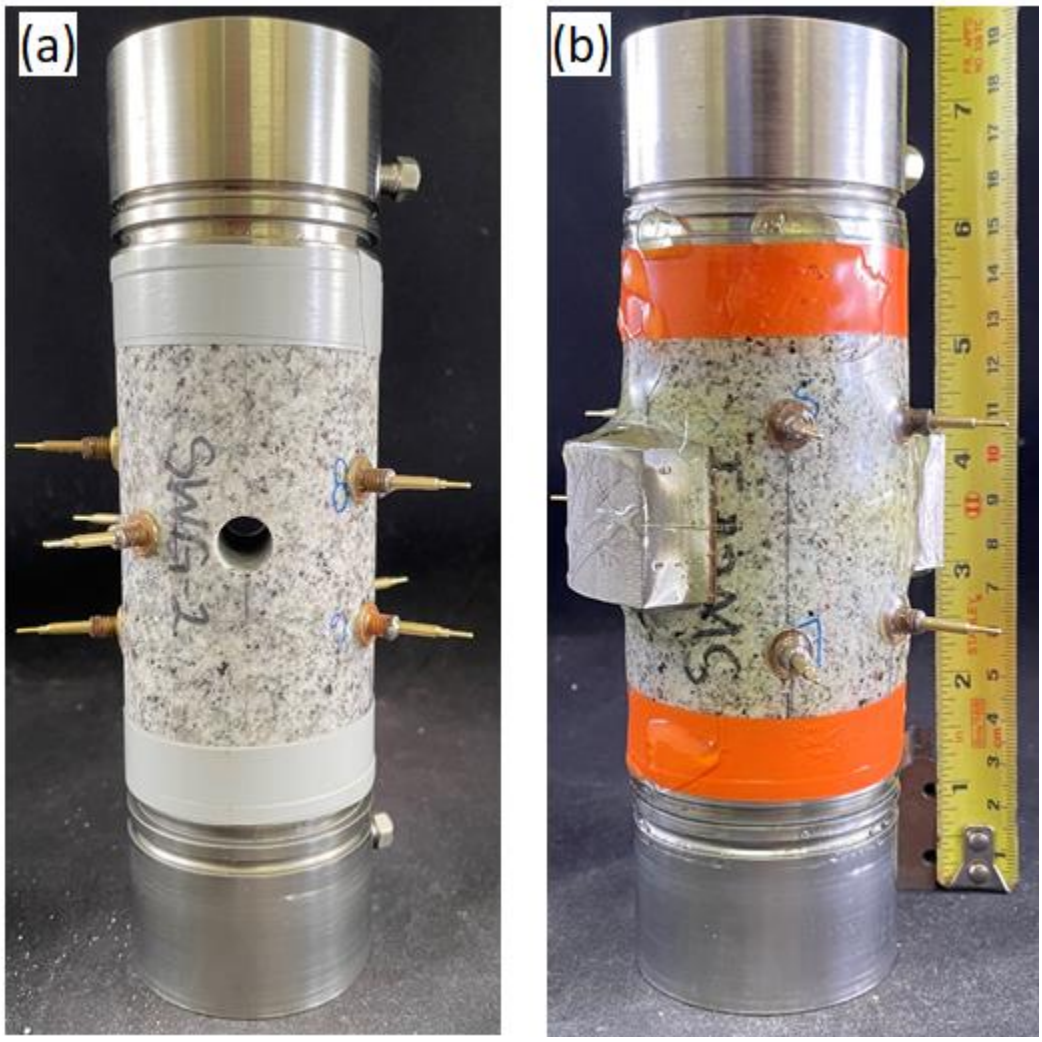

Figure 5. Specimen preparation: (a) simulated borehole in Sierra White granite; (b) jacketed sample with borehole covers. A total of eight transducer pins are used to collect acoustic emission signal.

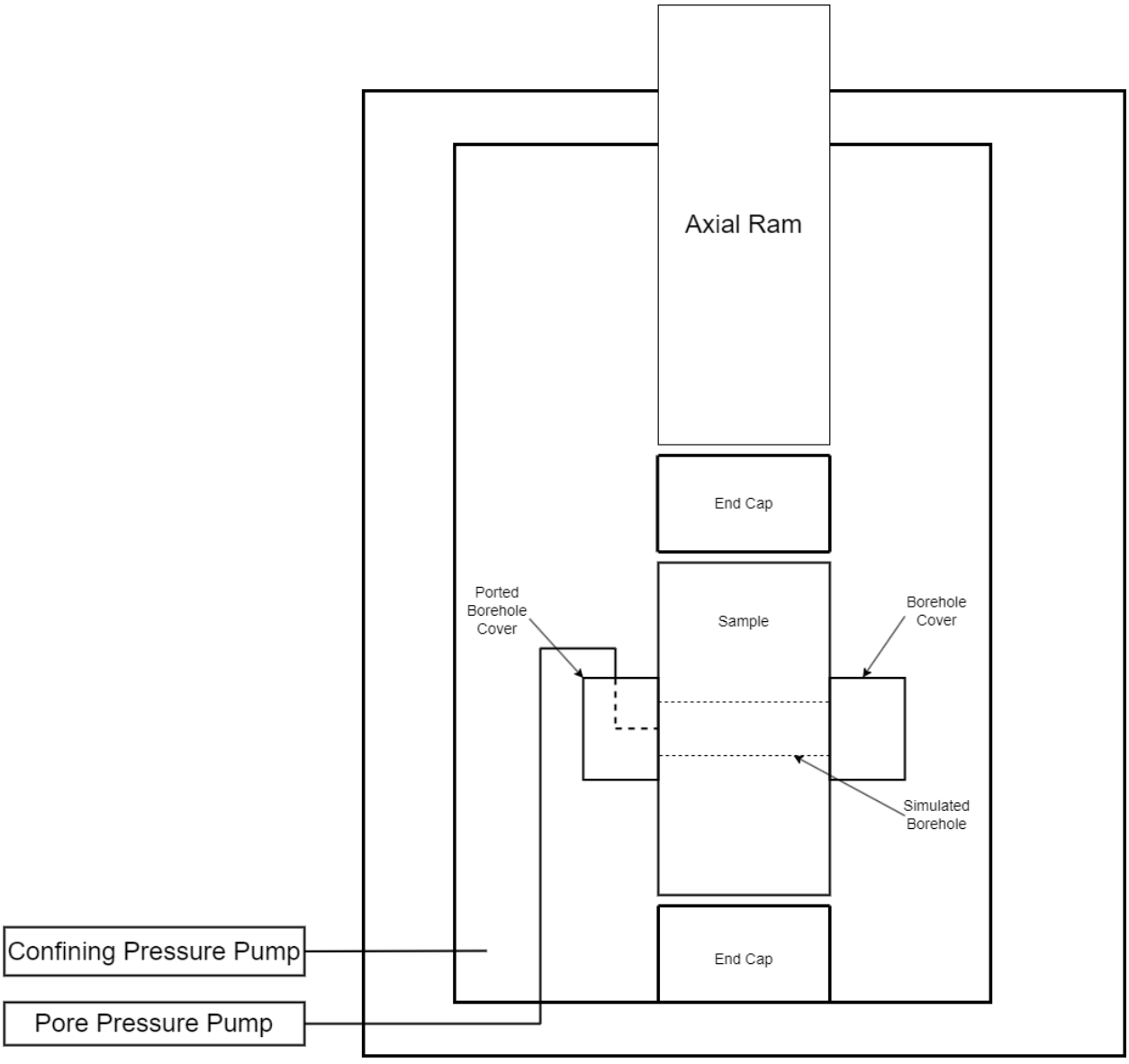

Figure 6. Experimental setup for borehole simulation tests.

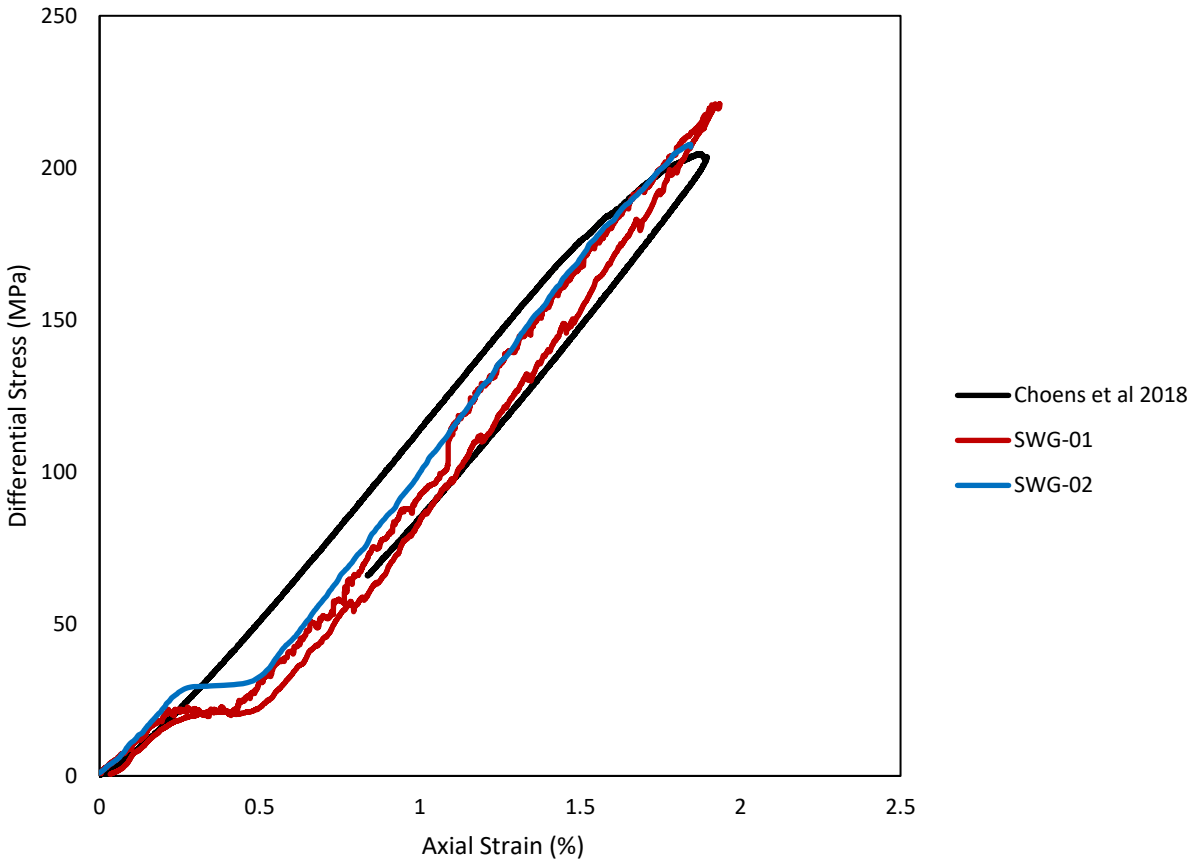

Figure 7. Differential stress versus axial strain for two testing in this work compared to the previously performed one in Choens et al. (2018).

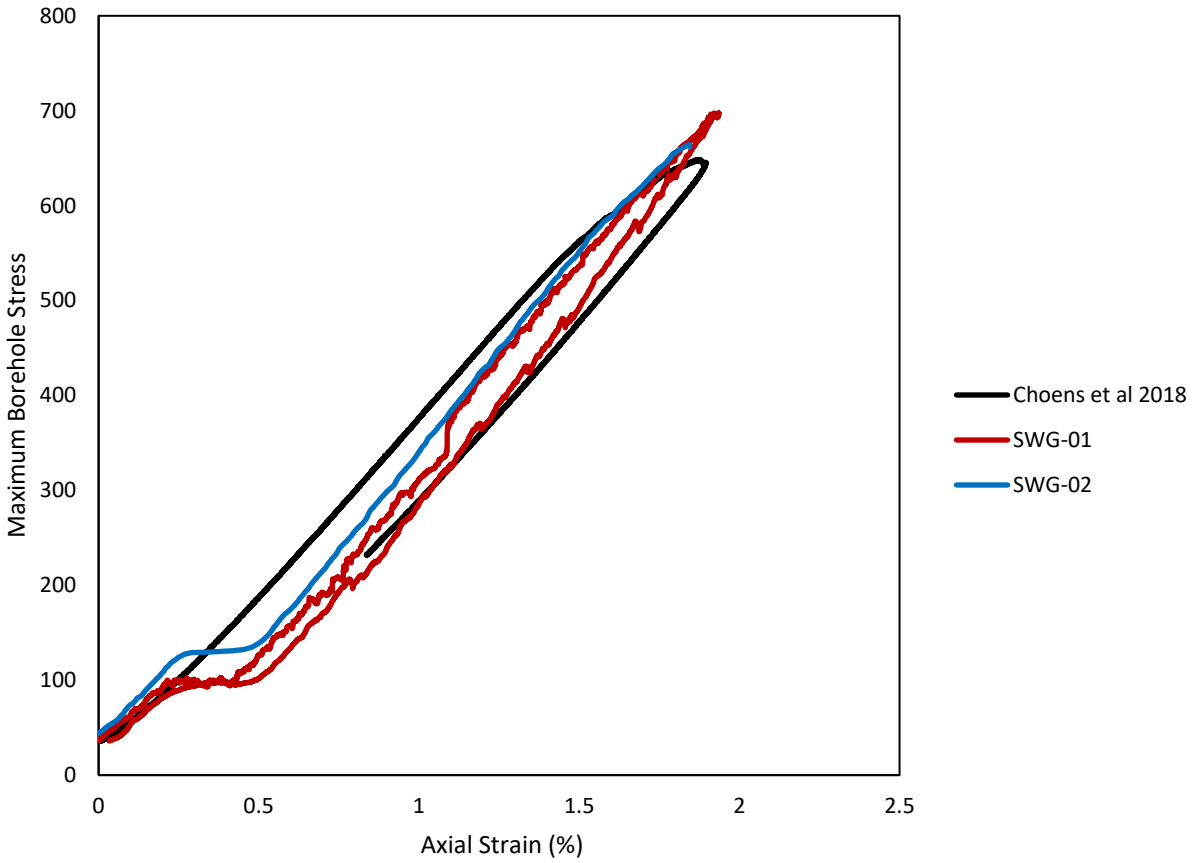

Figure 8. Maximum borehole stress, σ_{BH}, versus axial strain.

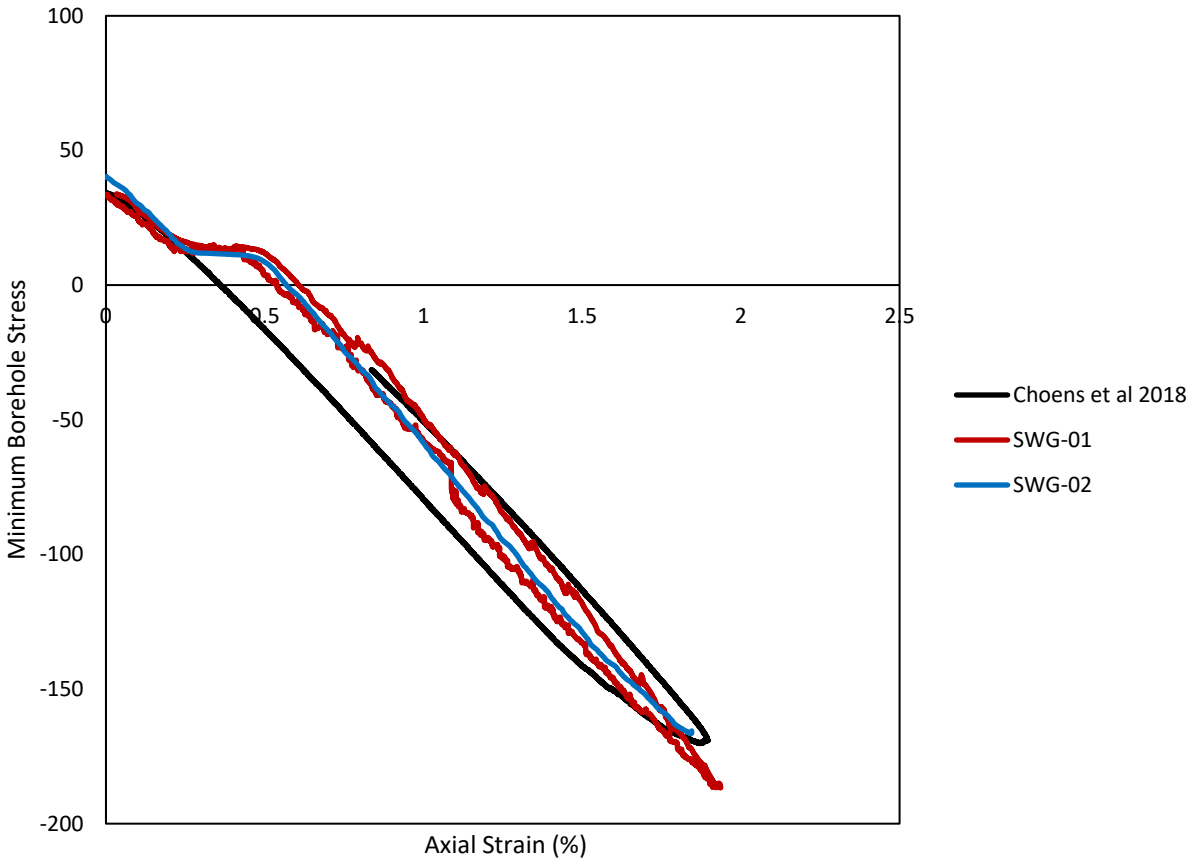

Figure 9. Minimum borehole stress, σ_{BV}, versus axial strain.

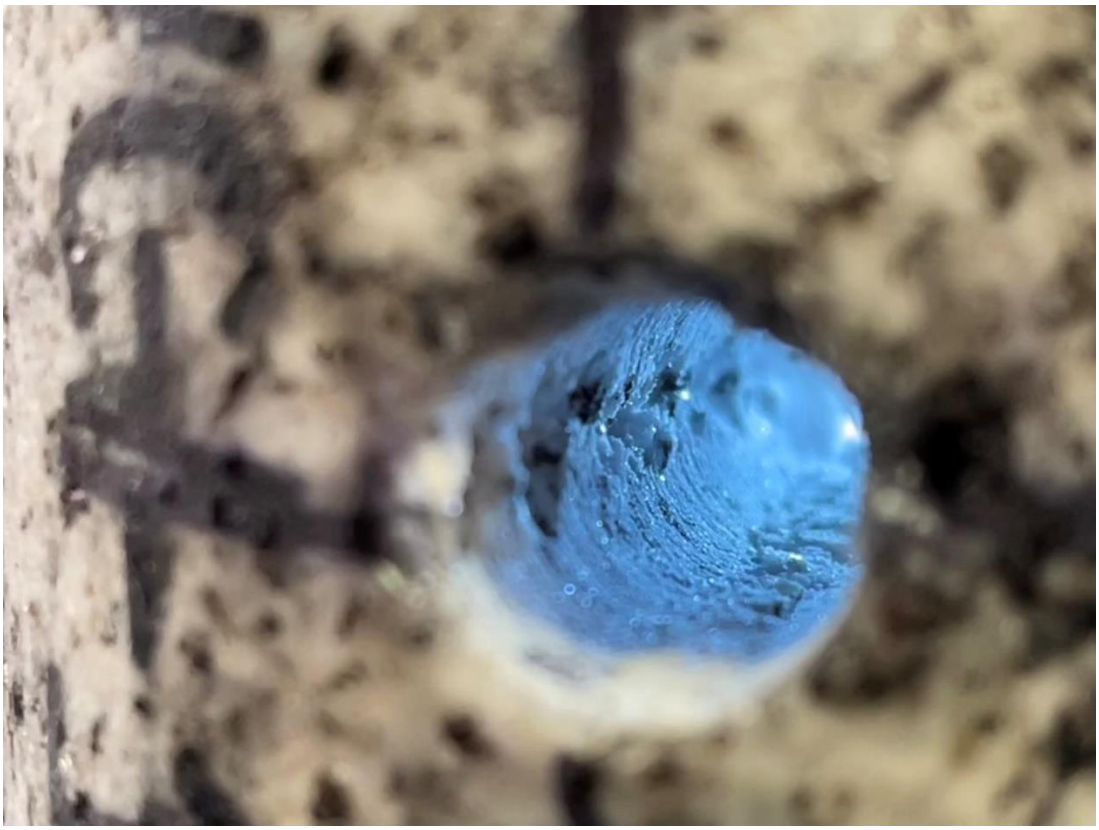

Figure 10. Borehole of sample SWG-01 after deformation. Fracturing occurs along the horizontal plane of the borehole.

Appendix. List of experimental data files

Experimental data in this report are available as followings:

1. Triaxial Shear Tests on Simulated Sierra White Fault Gouge
    - Sierra White Granite Gouge Friction Tests_15 MPa Gouge Test.csv
    - Sierra White Granite Gouge Friction Tests_75MPa DRY Gouge Test.csv
    - Sierra White Granite Gouge Friction Tests_75MPa DI H2O Gouge Test.csv
2. 2. Borehole Stimulation Experiment
    - Borehole_SWG01.csv
    - Borehole_SWG02.csv
    - Borehole_Previous Borehole Data.csv

Acknowledgment: Sandia National Laboratories is a multimission laboratory managed and operated by National Technology & Engineering Solutions of Sandia, LLC, a wholly owned subsidiary of Honeywell International Inc., for the U.S. Department of Energy's National Nuclear Security Administration under contract DE-NA0003525.